BOLETÍN DE LOS OBSERVATORIOS DE TONANTZINTLA Y TACUBAYA, VOL. 5, N°35, 1970.

BVRI—PHOTOMETRY OF THE BRIGHTEST STARS IN THE MAGELLANIC CLOUDS

Eugenio E. Mendoza V.

SUMARIO

La fotometría en el sistema *BVRI* de cien objetos que pertenecen a una u otra de las dos Nubes de Magallanes, indica dos notables diferencias entre ellos y las estrellas supergigantes de la Galaxia: Algunas estrellas de las Nubes de Magallanes son más luminosas que las más luminosas supergigantes galácticas. Además las estrellas de las Nubes tienen un exceso en el color *V—R* que no puede explicarse solamente por extinción interestelar. Las causas más probables de esta última propiedad son: O una envolvente circunestelar de polvo o una composición química en sus atmósferas diferente a la de las supergigantes de la Vía Láctea, o quizás ambas causas.

ABSTRACT

We have made photometric observations in the *BVRI* system of 100 objects that belong to the Magellanic Clouds. The observational data indicate at least two remarkable differences between some of the Magellanic Cloud objects and the supergiant stars in the Galaxy, namely, the former are more luminous than the most luminous galactic supergiants and they also have a color excess in *V—R* unexplained by interstellar extinction alone. Two possible explanations are likely for the additional color excess; either the presence of a circumstellar dust envelope or a different chemical atmospheric composition from galactic supergiant stars, or perhaps both of them.

I. Introduction

To understand better star formation and stellar evolution, it is necessary to study stars and their environment under very different conditions. One way to accomplish this matter could be observing individual stars in galaxies of different nature. So far this has been a difficult task and thus, the present knowledge of star formation and stellar evolution is based practically only in observations of the stars of the Galaxy. A number of individual objects has been observed in other galaxies, mostly the Andromeda Nebula and the Magellanic Clouds. Studies made of the Magellanic Cloud stars show that several of them have luminosities much higher than the most luminous supergiant galactic stars so far known (cf. Mendoza 1969*b*). This observational fact raises many questions.

To study the nature of the brightest stars in the Magellanic Clouds we have planned to make multicolor photometry of these objects. This paper shows the *BVRI*-photometry of 100 objects, 25 belong to the Small Magellanic Cloud and 75 belong to the Large Magellanic Cloud. The observations were obtained with the 36 and 60-inch telescopes of the Cerro Tololo Inter-American Observatory* from November 13 to December 3, 1969. The study is not complete since we hope to obtain infrared measurements (1-5 microns) soon. However the observational data presented here show results which by themselves are very interesting.

II. The Observations

The observational data on the *BVRI*-photometric system defined by Johnson (1964) have been obtained using the very same *B, V, R, I* filters used at Tonantzintla Observatory (Mendoza 1963, 1967*b*, 1967*c*) and an RCA 7102 as the only detector employed in the observations. Four stars have been added to Tonantzintla standard stars to obtain better results in the transformations and the atmospheric extinction coefficients. Table 1 lists the standard stars used in this program. The columns of this Table contain: first, the Bright Star (BS) Catalogue number (Hoffleit 1964); second, the name of the star; third, the spectral type (mostly MK); fourth through seventh, the *V* magnitude and the *B—V, V—R,* and *R—I* color indices, respectively; and, last, the number of different nights in which the standard stars were observed. The actual number of standard star observations is larger by approximately a factor of 3.

The extinction coefficients were computed using the formula:

$$K_C = k + k' \times C$$

where

$C = V,\ B-V,\ V-R,$ or $R-I$
$k' = 0$ for $C \neq B-V$
$k' = -0.033$ for $C = B-V$

* Telescope time at Cerro Tololo Inter-American Observatory was granted according to an agreement between AURA, Inc. and the University of Chile.

TABLE 1

Standard Stars

BS	*Name*	*Sp*	*V*	*B–V*	*V–R*	*R–I*	*n*
497	π Scl	gK0	5.25	+1.05	+0.80	+0.54	20
498		A2 V	5.71	−0.01	+0.05	−0.01	20
718	ξ^2 Cet	B9 III	4.29	−0.06	+0.03	−0.05	14
753		K3 V	5.82	+0.97	+0.84	+0.53	14
875		A1 V	5.17	+0.08	+0.11	+0.06	14
1084	ε Eri	K2 V	3.73	+0.88	+0.72	+0.47	10
1855	υ Ori	B0 V	4.63	−0.26	−0.11	−0.26	14
1958		gK0	5.44	+0.91	+0.71	+0.47	20
1996	μ Col	09.5 V	5.17	−0.28	−0.11	−0.27	20
3249	β Cnc	K4 III	3.52	+1.48	+1.13	+0.78	4
3454	η Hya	B3 V	4.30	−0.20	−0.06	−0.19	4

Table 2 gives the mean k-coefficient for *B, V, R,* and *I*. However, they were not employed in the reductions since in the actual computations we use the individual values obtained each night.

TABLE 2

Observed Atmospheric Extinction
(Nov 13 - Dec 3, 1969)

Filter Band	λ_o (μ)	*k*
B	0.44	0.240
V	0.55	0.143
R	0.70	0.089
I	0.90	0.060

The broad band *BVRI*-photometry of 100 objects that belong to either one or another of the Magellanic Clouds is given in Tables 3a, 3b and 4. Table 3a gives the observational data for the Small Magellanic Cloud. The columns of this Table contain, first, the Radcliffe serial number (Feast, Thackeray, and Wesselink 1960); second, the HD number or other designation (HV, Harvard variable, Arp (Arp 1958), Hen (Henize 1956)); third through sixth, the mean *V* magnitude and *B–V, V–R,* and *R–I* color indices, respectively; seventh, the number of independent observations of each star; eighth, the spectral type given by Feast *et al.* (1960); and last, the radial velocity (Feast *et al.* 1960). In Table 3a two stars not given by Feast *et al.* (1960) have been added (W1 and W3). They were taken from Westerlund, Danziger, and Graham (1963). The spectral types and radial velocities are also taken from these authors. Table 3b gives the observational data for the Large Magellanic Cloud. The columns of this Table are the same as those of Table 3a. As we stated before Table 3 gives mean photometric values. They were obtained as the arithmetic mean of the individual observations. These values are listed in Table 4. The columns of Table 4 list: first, the number given in column 1 of Table 3 (a and b); second through fifth, each one of the *BVRI*-observations; sixth, the size of the diaphragm used in the focal plane of both telescopes (20″ with the 60-inch and 35″.2 with the 36-inch telescopes); last, the Julian Day.

A number of stars listed in Tables 3 and 4 are variable stars or are suspected of variability, yet they show only small variations, if any. S Dor (R 88) shows the largest light variability: ΔV = 0.14 mag. $\Delta\ (B-V)$ = 0.05 mag. $\Delta\ (V-R)$ = 0.11 mag. and $\Delta\ (R-I)$ = 0.06 mag. Its light curves, in four wavelength regions, are shown in Figures 1-4. The plotted difference in magnitudes is the mean magnitude minus the observed magnitude. The curves are smooth and show roughly how the star became brighter every night; yet on November 16, apparently, S Dor had a flare up of nearly 0.16 mag. in the blue (largest value), and of approximately 0.04 mag. in the red (smallest value).

It has been shown (Mendoza 1970) that variable sky background may affect the quality of the observational data. Thus, it is interesting to compare our photometry with that obtained by

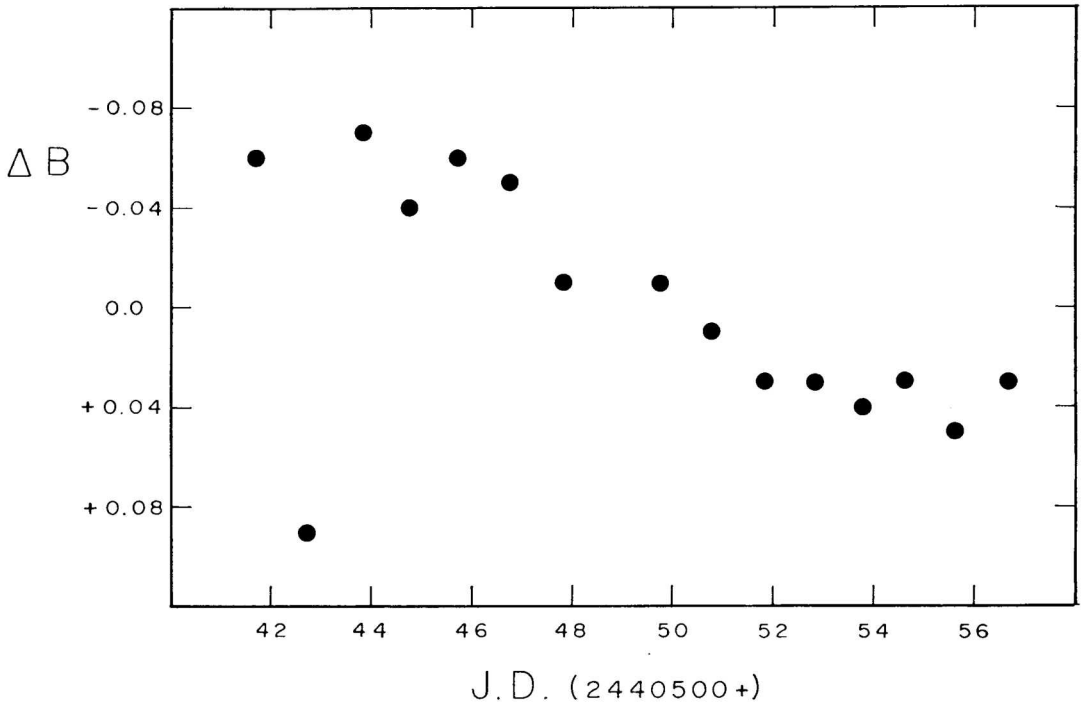

Fig. 1.—*Light curve of S Dor in blue light.*

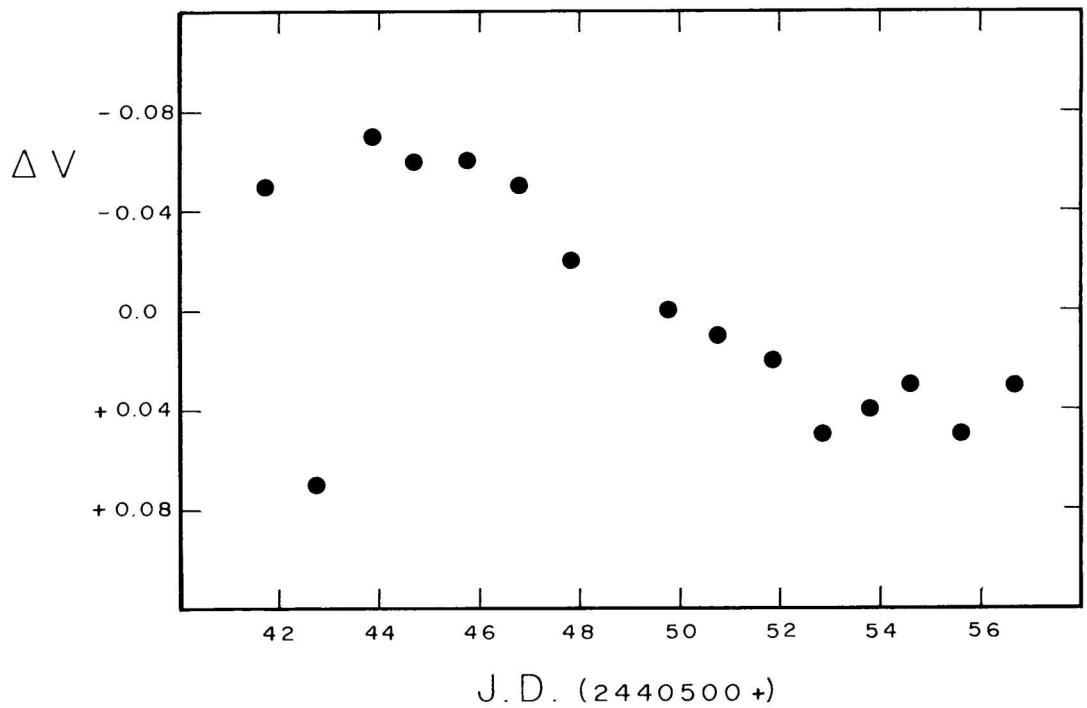

Fig. 2.—*Light curve of S Dor in yellow light.*

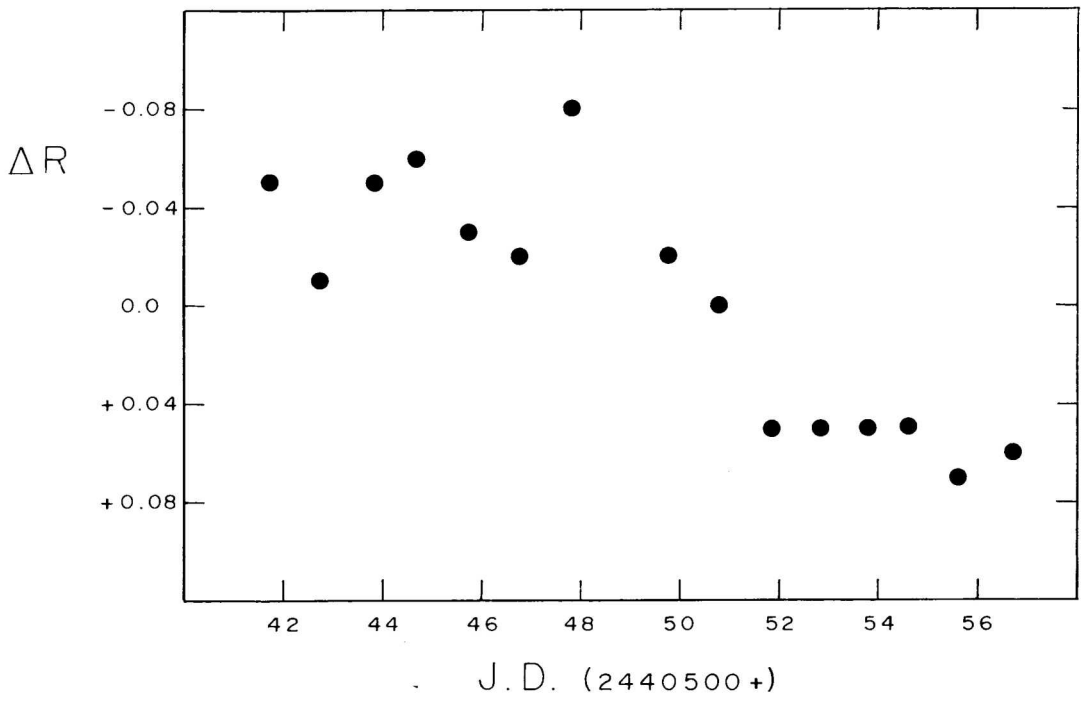

Fig. 3.—*Light curve of S Dor in red light.*

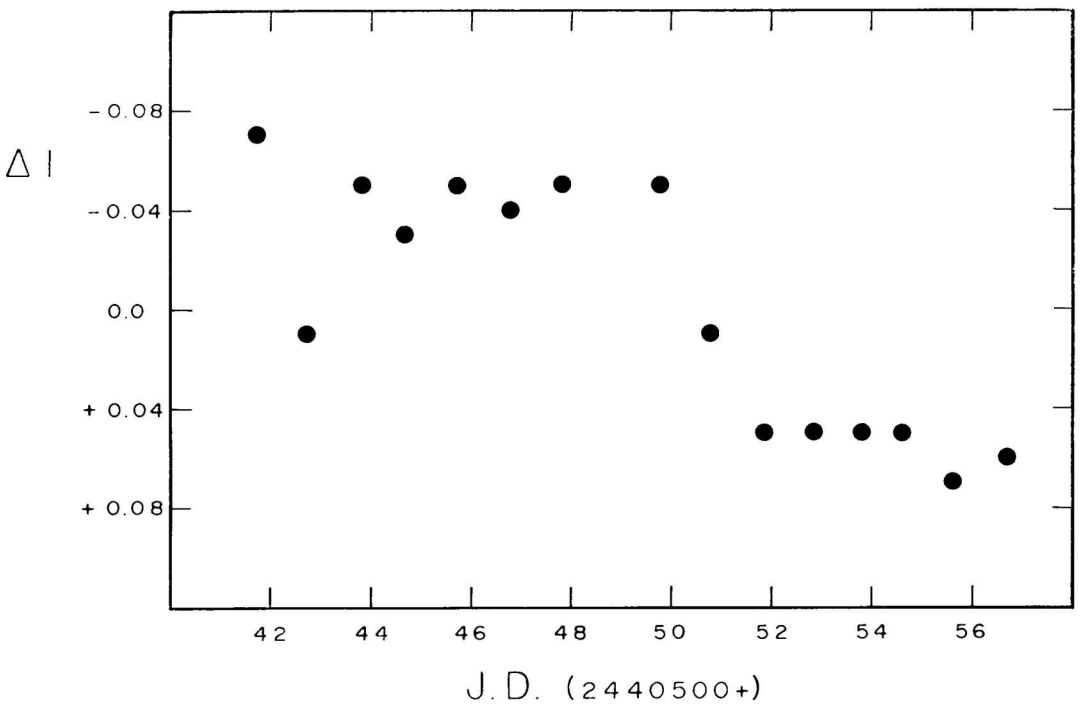

Fig. 4.—*Light curve of S Dor in infrared light. (around 9/10 microns).*

TABLE 3*a*

BVRI-Photometry of Members of the Small Magellanic Cloud

Radcliffe	*Star*	*V*	*B–V*	*V–R*	*R–I*	*n*	*Sp*	*R. V.*
1	HV 821	11.68	+0.84	+0.65	+0.46	5	F8 Ia	
5	4862	10.96	−0.05	+0.09	−0.03	3	B3 I	+152
6	4976	11.00	+0.14	+0.13	+0.08	3	B6 I	+168
7	HV 829	12.18	+0.53	+0.45	+0.30	4	G0: I	
8	5030	11.17	+0.12	+0.09	+0.16	3	A0 Ia:	+168
9	5045	11.01	+0.01	+0.06	−0.02	3	B3 Ia:	+168
10	5277	10.93	+0.12	+0.16	+0.16	3	A0 Ia:	+139
11	5291	10.79	+0.05	+0.08	+0.06	3	B6 Ia	+158
14	5980	11.66	−0.18	−0.10	−0.26	1	Wp	
19	Arp g	11.59	+0.15	+0.19	+0.23	3	A3 Ia	+169
21		11.53	+0.02	+0.27	+0.05	2	A0 Ia:	+120
23		12.13	−0.02	+0.06	−0.02	2	A1 I	+149:
26		11.55	+0.27	+0.30	+0.28	3	F0 Ia:	+178
27		10.89	+0.09	+0.18	+0.07	4	B9 Ia	+143
36	Arp e	11.32	0.00	+0.09	−0.03	3	B3 I	+196
37	Arp b	11.19	+0.08	+0.20	+0.04	3	B6 I	+180
39	Hen S45	11.50	−0.01	+0.08	−0.03	2	B2: I(e)	+144:
40	6884	10.67	+0.08	+0.34	+0.04	3	B8 Ie	+181
42	7099	10.95	−0.04	+0.06	−0.06	3	B2.5 I	+247
43	Arp d	11.32	+0.12	+0.17	+0.18	3	A3 I	+175
45	7583	10.16	+0.14	+0.19	+0.17	2	A0 Ia-0	+175
47	Hen S63	11.61	+0.38	+0.34	+0.23	3	F Ie	+121:
50	Hen S65	11.54	+0.19	+0.58	+0.06	3	Pec	+184
W1		11.87	−0.05	+0.10	−0.04	2	B0 I	+149
W3		11.78	0.00	+0.17	+0.03	2	B3 Ia	+165

TABLE 3*b*

BVRI-Photometry of Members of the Large Magellanic Cloud

Radcliffe	*Star*	*V*	*B–V*	*V–R*	*R–I*	*n*	*Sp*	*R. V.*
51	270754	11.27	+0.10	+0.20	+0.05	2	B1.5 Ia:	+306
52	268654	10.53	+0.16	+0.18	+0.14	4	B8 I	+266
53	268605	11.35	−0.12	−0.04	−0.11	2	B0 Ia	+309
54	31673	12.63	+0.09	+0.68	−0.36	3	Neb	+250
55	268718	10.72	+0.24	+0.28	+0.27	3	B9 Ieq	+268
56	268326	11.56	−0.04	+0.05	−0.05	2	B2 Ia	+312
57	268653	10.73	−0.02	+0.08	−0.05	3	B3 I	+301
58	268729	10.99	+0.11	+0.24	+0.09	3	B5 I	+271
59	268757	10.24	+1.53	+1.04	+0.68	3	G5 Ia	+258
61	268675	10.81	+0.04	+0.14	+0.03	2	A0 Ia	+286
62	32034	9.66	+0.10	+0.17	+0.06	3	B9 Ie	+295
64	32228	10.81	−0.15	−0.02	−0.13	4	WC6 + 08:	+275
65	268809	11.92	−0.06	+0.05	−0.13	3	B1 Ia:	+258
66	268835	10.63	+0.15	+0.37	+0.13	3	Aeq	+271(e); +54(a)
67	32763	11.43	+0.22	+0.81	+0.95	3	Pec	+244
68	270933	10.98	0.00	+0.09	+0.02	3	B8 I	+313
70	270949	11.16	−0.09	+0.06	−0.03	2	B3 I	+300

TABLE 3*b* (continued)

Radcliffe	*Star*	*V*	*B–V*	*V–R*	*R–I*	*n*	*Sp*	*R. V.*
71	269006	10.54	+0.05	+0.13	+0.05	4	B2.5 Iep	+192(e); +198(a)
72	268993	11.99	+0.03	+0.10	+0.02	3	A0 Ia	+237
73	268907	10.62	0.00	+0.12	+0.01	3	B8 Ia	+305
74	268939	10.95	+0.10	+0.19	+0.06	3	B Ie	+299
75	268946	10.31	+0.09	+0.17	+0.09	3	A0 Ia	+297
76	33579	9.13	+0.19	+0.23	+0.15	3	A3: Ia-0 (e)	+253
78	269050	11.70	−0.07	+0.08	−0.09	2	B0 Ia	+238
80	269172	10.61	+0.07	+0.22	+0.09	3	A0 Ia-0	+231
81	269128	10.41	0.00	+0.23	0.00	3	B2.5 Ieq	+227
82	269217	11.88	+0.06	+0.43	−0.07	3	Pec	+236
84	269227	11.79	+0.20	+0.75	+1.05	3	Pec	+262:(e); +28:(a)
85	269321	10.83	+0.09	+0.32	+0.09	3	B5 Iae	+292
86	35342	10.10	−0.11	−0.06	−0.13	3	Cluster	
87	269333	11.22	−0.09	+0.02	−0.12	1	W + B1 : I	+286
88	35343	10.76	+0.02	+0.29	−0.01	15	Aeq	+295(e); +213(a)
89 + 90	35517	10.85	−0.19	+0.06	−0.10	2	B0 I + WC 6:	+285
92	271182	9.71	+0.58	+0.53	+0.31	3	F8 Ia	+322
94	271191	10.06	+0.76	+0.99	+0.84	3	B comp.	+291
98	271192	10.58	+0.12	+0.14	+0.15	3	A0 Ia-0:	+308
99	269445	11.45	+0.25	+0.56	+0.20	2	Pec	+278
100	269475	11.56	−0.01	+0.09	+0.09	3	B3 I	+251
101	269547	11.60	+0.06	+0.12	+0.04	3	B3 Ia:	+251
103	269546	9.90	−0.02	+0.10	0.00	3	B3 Ip	+298
104	271279	11.26	+0.09	+0.16	+0.11	3	A0 Ia:	+306
105	269599	10.02	+0.21	+0.62	+0.64	3	Cluster	+268
107	269644	11.18	−0.01	+0.08	−0.04	2	B6 Ia	+336
110	269662	10.41	+0.24	+0.32	+0.18	3	B9: Ieq	
111	269661	10.33	+0.12	+0.18	+0.13	3	B9 Ia-0	+260
112	269660	11.16	−0.02	+0.07	−0.07	3	B2 Ia	+237
113	269676	11.47	−0.11	0.00	−0.07	3	06e	+244:
116	269700	10.54	0.00	+0.16	0.00	3	B1.5 Iacq	+252
117	269723	9.93	+1.04	+0.76	+0.53	3	G0 Ia	+317
118	269781	9.88	+0.07	+0.13	+0.07	4	A0 Iae	+342
119	269787	10.81	+0.11	+0.20	+0.12	2	A0 Ia-0	+312:
120	269797	10.89	+0.04	+0.13	+0.07	3	B8 Ia-0:	+288
121	269801	10.51	+0.08	+0.14	+0.06	3	B9 Ia-0	+319
123	37836	10.65	+0.11	+0.45	+0.11	3	Pec	+267
124	269841	11.87	+0.10	+0.24	+0.14	2	A0	
125	269845	11.78	−0.02	+0.11	−0.05	2	B3 I	+292
126	37974	10.94	+0.15	+0.70	−0.06	3	Pec	+258
127	269858	11.16	−0.07	+0.17	−0.13	3	Pec	+284
128	269859	10.48	−0.06	+0.03	−0.06	3	B1 I	+268
129	269896	11.32	+0.91	+0.11	−0.08	2	B0 Ia	+273
130	269891	11.34	+0.17	+0.18	+0.11	3	B0: + W?	
131	269902	10.21	+0.37	+0.40	+0.30	3	B9 I	+269
136	38268	9.15	+0.17	+0.32	+0.21	3	O + WN	+274
144	38283	11.11	−0.12	+0.14	0.00	2	WN 7	
148	−69°474	11.94	+0.26	+0.51	+0.22	2	B5I + Neb	

TABLE 3*b* (continued)

Radcliffe	*Star*	*V*	*B–V*	*V–R*	*R–I*	*n*	*Sp*	*R. V.*
149	−69°476	12.27	−0.05	+0.20	−0.18	3	Be + Neb	
150	269953	9.94	+0.88	+0.72	+0.43	3	G0 Ia	+241
151	269982	10.74	+0.35	+0.33	+0.33	2	A5 Ia:	
152	269992	11.20	+0.05	+0.16	+0.05	2	B2.5 Ia	+258
153	270086	10.30	+0.25	+0.28	+0.21	4	A1 Ia-0:	+253
154	270151	12.00	+0.10	+0.18	+0.08	3	B1 I	+242
155	270196	11.61	−0.07	+0.07	−0.10	2	B1.5 Ia	+248
156	268807	11.63	−0.06	+0.28	+0.31	2	Cluster	
156	268807	11.78	+0.06	+0.06	0.00	2	Cluster	
157	268820	10.84	+0.26	+0.44	+0.54	2	Cluster	
157	268820	11.11	+0.23	+0.43	+0.64	2	Cluster	
158	269578	10.02	+0.16	+0.50	+0.53	2	Cluster	
158	269578	10.25	+0.27	+0.57	+0.65	2	Cluster	

other observers. Figures 5 and 6 illustrate graphically a comparison between the *V, B* – photometry given in Table 3 and that by Feast *et al.* (1960). This comparison indicates a possible systematic difference between both visual magnitudes, smaller than 0.02 mag., and none in the B–V color indices. The internal accuracy has a mean error smaller than 0.02 mag. in *V, B–V, V–R,* and *R–I.* In this estimate we eliminated only the well known variable stars. If we also exclude stars suspected of light variability, then the mean errors are even lower.

TABLE 4

Journal of Observations of Magellanic Cloud Objects

Star	*V*	*B–V*	*V–R*	*R–I*	D(″)	J. D. 2440500+
1	11.68	+0.82	+0.64	+0.45	20	49.522
1	11.70	+0.80	+0.66	+0.46	20	50.522
1	11.70	+0.87	+0.65	+0.46	20	51.583
1	11.67	+0.86	+0.65	+0.45	20	53.519
1	11.67	+0.84	+0.65	+0.47	20	54.533
5	10.97	−0.05	+0.10	−0.02	35	39.569
5	10.96	−0.06	+0.08	−0.05	35	41.532
5	10.95	−0.04	+0.09	−0.02	35	43.542
6	10.97	+0.16	+0.11	+0.07	35	39.553
6	11.00	+0.14	+0.15	+0.08	35	41.548
6	11.02	+0.13	+0.13	+0.09	35	43.557
7	12.19	+0.52	+0.44	+0.26	20	50.538
7	12.18	+0.54	+0.45	+0.33	20	53.532
7	12.17	+0.52	+0.45	+0.30	20	54.543
7	12.18	+0.53	+0.46	+0.30	20	55.527
8	11.14	+0.06	+0.09	+0.20	35	39.534
8	11.24	+0.17	+0.08	+0.16	35	40.544
8	11.14	+0.12	+0.11	+0.13	35	42.527
9	10.99	0.00	+0.05	0.00	35	39.518
9	10.99	+0.03	+0.06	−0.04	35	40.524
9	11.04	0.00	+0.07	−0.02	35	42.541

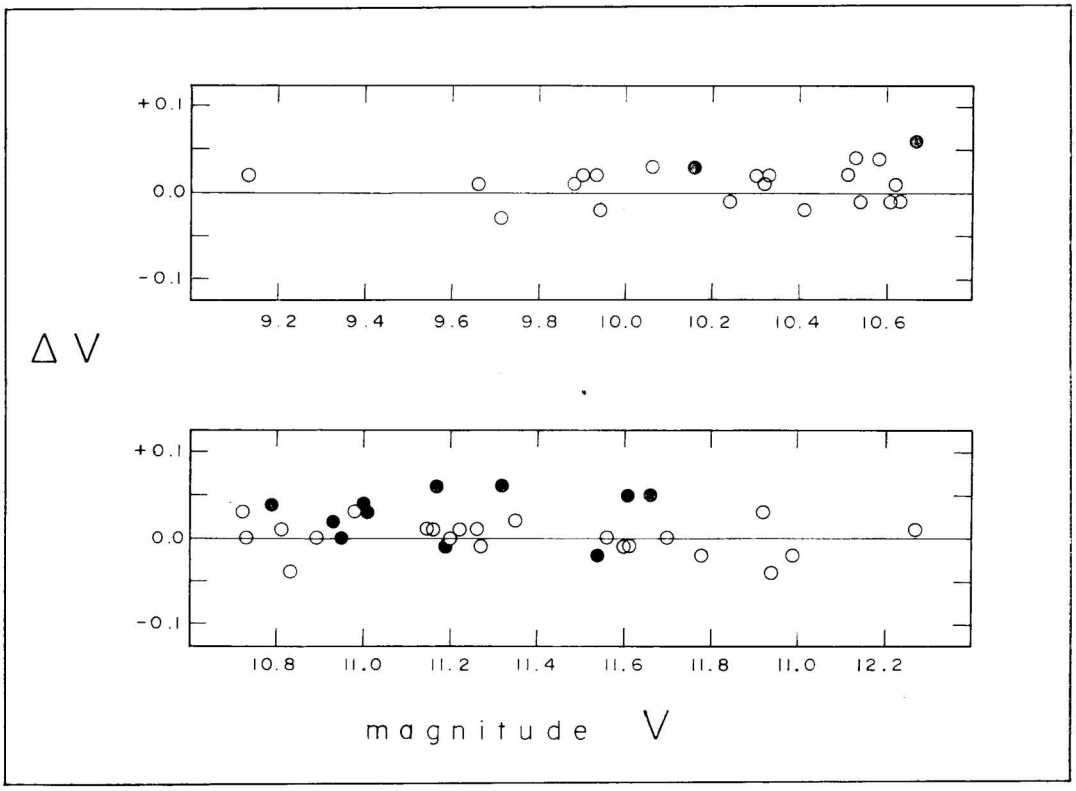

Fig. 5.—*Comparison between the* V *given in Table 3 and the* V *given by Feast* et al *(1960). The circles represent the difference between* V *(Table 3) and V (Feast). Filled circles represent members of the Small Magellanic Cloud, and open circles represent members of the Large Magellanic Cloud.*

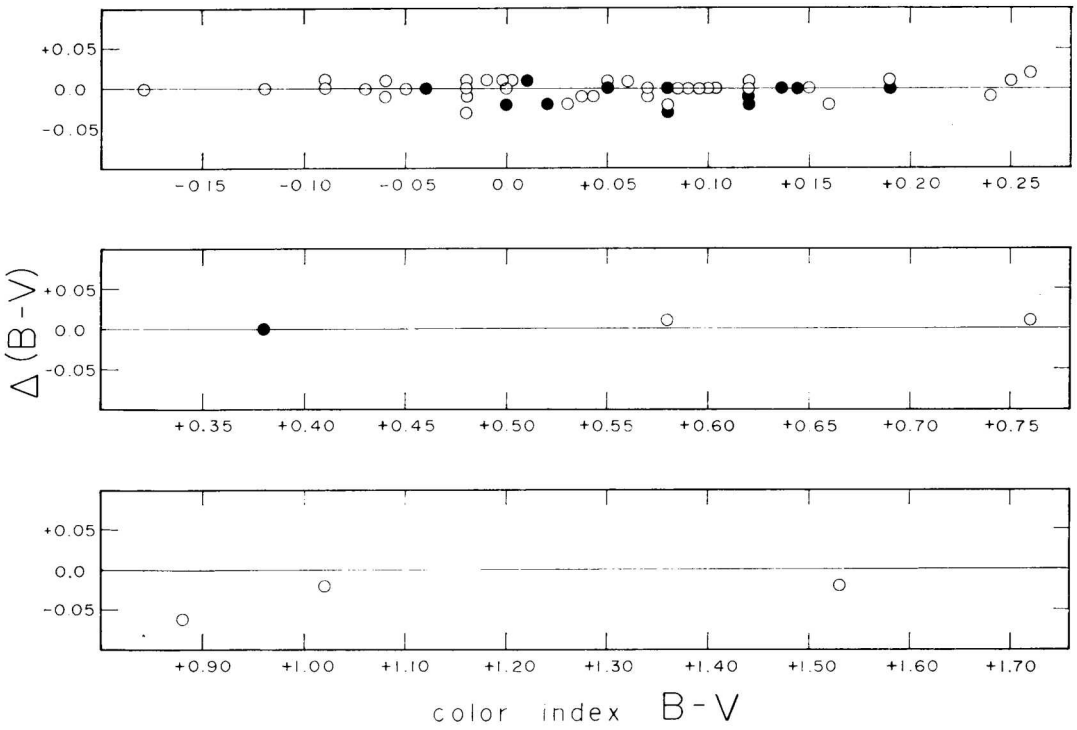

Fig. 6.—*Comparison between the* B—V *given in Table 3 and the* B—V *given by Feast* et al *(1960). The circles represent the difference between* B—V *(Table 3) and* B—V *(Feast). Filled circles, represent members of the Small Magellanic Cloud, and open circles represent members of the Large Magellanic Cloud.*

TABLE 4 (continued)

Star	*V*	*B–V*	*V–R*	*R–I*	D(″)	J. D. 2440500+
10	10.97	+0.08	+0.17	+0.17	35	39.602
10	10.90	+0.13	+0.15	+0.15	35	41.566
10	10.93	+0.14	+0.16	+0.16	20	46.533
11	10.78	+0.07	+0.06	+0.09	35	40.567
11	10.80	+0.04	+0.10	+0.05	35	41.588
11	10.80	+0.05	+0.08	+0.05	20	47.545
14	11.66	−0.18	−0.10	−0.26	35	43.604
19	11.60	+0.15	+0.20	+0.23	20	45.569
19	11.59	+0.16	+0.18	+0.24	20	46.569
19	11.59	+0.15	+0.20	+0.22	20	49.552
21	11.51	+0.02	+0.25	+0.07	20	55.537
21	11.55	+0.02	+0.29	+0.03	20	56.523
23	12.12	0.00	+0.06	−0.02	20	55.548
23	12.14	−0.04	+0.06	−0.02	20	56.533
26	11.55	+0.26	+0.30	+0.28	20	53.545
26	11.55	+0.26	+0.30	+0.29	20	54.566
26	11.55	+0.28	+0.29	+0.27	20	56.543
27	10.90	+0.09	+0.17	+0.09	35	39.659
27	10.87	+0.10	+0.18	+0.07	35	41.608
27	10.89	+0.10	+0.18	+0.05	35	42.559
27	10.89	+0.06	+0.18	+0.06	35	44.588
36	11.33	0.00	+0.09	−0.03	20	45.614
36	11.32	+0.02	+0.08	−0.03	20	47.615
36	11.32	−0.02	+0.10	−0.03	20	50.584
37	11.20	+0.08	+0.20	+0.04	20	45.628
37	11.18	+0.05	+0.20	+0.04	20	47.668
37	11.19	+0.11	+0.21	+0.04	20	50.596
39	11.50	−0.01	+0.09	−0.03	20	53.584
39	11.50	−0.01	+0.07	−0.03	20	54.576
40	10.67	+0.06	+0.35	0.00	35	40.580
40	10.66	+0.10	+0.33	+0.04	35	43.644
40	10.69	+0.09	+0.34	+0.08	20	49.578
42	10.93	−0.01	+0.02	−0.05	35	40.594
42	10.96	−0.05	+0.06	−0.06	35	42.590
42	10.96	−0.04	+0.10	−0.07	20	49.602
43	11.32	+0.12	+0.17	+0.17	20	46.600
43	11.31	+0.13	+0.17	+0.17	20	47.562
43	11.33	+0.11	+0.18	+0.19	20	50.554
45	10.16	+0.14	+0.19	+0.17	35	42.605
45	10.16	+0.14	+0.19	+0.17	20	44.616
47	11.62	+0.38	+0.34	+0.22	20	46.627
47	11.61	+0.38	+0.34	+0.23	20	47.590
47	11.60	+0.38	+0.34	+0.23	20	49.617

TABLE 4 (continued)

Star	*V*	*B–V*	*V–R*	*R–I*	D(″)	J. D. 2440500+
50	11.54	+0.19	+0.57	+0.06	20	46.645
50	11.52	+0.20	+0.58	+0.06	20	47.649
50	11.56	+0.18	+0.58	+0.06	20	50.620
W1	11.87	−0.04	+0.10	−0.04	20	55.573
W1	11.87	−0.06	+0.10	−0.04	20	56.565
W3	11.79	−0.01	+0.18	+0.02	20	55.583
W3	11.77	+0.01	+0.16	+0.04	20	56.576
51	11.28	+0.09	+0.20	+0.04	20	51.651
51	11.26	+0.11	+0.19	+0.06	20	52.564
52	10.64	+0.10	+0.19	+0.13	35	39.702
52	10.53	+0.16	+0.18	+0.15	35	41.667
52	10.53	+0.16	+0.18	+0.14	35	43.676
52	10.42	+0.19	+0.17	+0.14	20	45.665
53	11.36	−0.12	−0.04	−0.11	20	51.664
53	11.34	−0.12	−0.04	−0.11	20	52.580
54	12.65	+0.12	+0.68	−0.36	20	51.681
54	12.62	+0.06	+0.66	−0.39	20	52.596
54	12.63	+0.09	+0.70	−0.34	20	56.588
55	10.73	+0.24	+0.28	+0.25	20	45.680
55	10.71	+0.26	+0.28	+0.25	20	46.675
55	10.72	+0.22	+0.29	+0.29	20	51.697
56	11.56	−0.04	+0.05	−0.06	20	51.720
56	11.56	−0.05	+0.05	−0.05	20	52.613
57	10.73	−0.03	+0.08	−0.05	20	47.667
57	10.73	−0.03	+0.08	−0.05	20	49.633
57	10.73	−0.01	+0.08	−0.05	20	50.633
58	11.00	+0.11	+0.24	+0.09	20	46.726
58	10.99	+0.10	+0.24	+0.09	20	47.684
58	10.98	+0.12	+0.24	+0.09	20	50.648
59	10.24	+1.50	+1.03	+0.68	35	40.668
59	10.24	+1.53	+1.04	+0.67	35	43.691
59	10.24	+1.55	+1.04	+0.68	20	51.735
61	10.80	+0.04	+0.14	+0.03	20	47.717
61	10.82	+0.04	+0.14	+0.03	20	52.638
62	9.66	+0.09	+0.17	+0.06	20	49.659
62	9.66	+0.10	+0.17	+0.06	20	50.660
62	9.66	+0.10	+0.17	+0.06	20	52.652
64	10.82	−0.14	−0.01	−0.13	20	49.675
64	10.81	−0.14	−0.02	−0.14	20	50.674
64	10.81	−0.17	−0.02	−0.13	20	51.763
64	10.81	−0.14	−0.03	−0.12	20	52.667
65	11.92	−0.07	+0.08	−0.15	20	52.682
65	11.92	−0.05	+0.04	−0.11	20	53.605
65	11.92	−0.06	+0.04	−0.11	20	56.597

TABLE 4 (continued)

Star	*V*	*B−V*	*V−R*	*R−I*	D(″)	J. D. 2440500+
66	10.64	+0.12	+0.37	+0.13	20	45.699
66	10.63	+0.16	+0.37	+0.13	20	46.690
66	10.62	+0.16	+0.37	+0.13	20	51.778
67	11.43	+0.21	+0.81	+0.95	20	52.699
67	11.43	+0.21	+0.81	+0.96	20	53.618
67	11.43	+0.18	+0.81	+0.94	20	56.607
68	10.98	0.00	+0.10	+0.01	20	49.691
68	10.98	0.00	+0.09	+0.02	20	50.689
68	10.98	−0.01	+0.09	+0.03	20	53.632
70	11.16	−0.09	+0.06	−0.03	20	52.715
70	11.16	−0.09	+0.06	−0.03	20	53.646
71	10.54	+0.05	+0.14	+0.06	20	46.796
71	10.53	+0.04	+0.13	+0.06	20	47.747
71	10.54	+0.05	+0.13	+0.04	20	47.770
71	10.54	+0.05	+0.13	+0.04	20	53.667
72	12.01	+0.02	+0.11	+0.01	20	52.729
72	11.99	+0.02	+0.10	+0.03	20	53.679
72	11.98	+0.05	+0.10	+0.03	20	56.620
73	10.62	+0.01	+0.12	+0.01	20	49.706
73	10.62	+0.01	+0.12	+0.01	20	50.703
73	10.62	−0.01	+0.12	+0.01	20	53.691
74	10.95	+0.10	+0.19	+0.05	20	49.721
74	10.95	+0.10	+0.19	+0.06	20	50.716
74	10.96	+0.10	+0.19	+0.06	20	53.703
75	10.31	+0.09	+0.18	+0.09	35	40.697
75	10.31	+0.09	+0.16	+0.09	35	43.741
75	10.31	+0.09	+0.17	+0.09	20	50.728
76	9.12	+0.20	+0.23	+0.15	35	40.710
76	9.13	+0.19	+0.24	+0.15	35	43.754
76	9.13	+0.19	+0.23	+0.16	20	51.791
78	11.71	−0.08	+0.08	−0.09	20	52.741
78	11.69	−0.06	+0.08	−0.09	20	53.716
80	10.61	+0.07	+0.21	+0.10	20	46.811
80	10.60	+0.07	+0.22	+0.09	20	47.787
80	10.61	+0.06	+0.23	+0.08	20	53.729
81	10.41	0.00	+0.23	0.00	35	40.735
81	10.41	0.00	+0.23	0.00	35	43.768
81	10.42	−0.01	+0.23	0.00	20	53.741
82	11.86	+0.05	+0.42	−0.06	20	52.780
82	11.91	+0.06	+0.44	−0.07	20	53.767
82	11.87	+0.06	+0.43	−0.08	20	56.630
84	11.81	+0.20	+0.75	+1.06	20	52.766
84	11.77	+0.20	+0.75	+1.04	20	53.778
84	11.79	+0.19	+0.74	+1.05	20	56.640

TABLE 4 (continued)

Star	*V*	*B–V*	*V–R*	*R–I*	D(″)	J. D. 2440500+
85	10.83	+0.08	+0.31	+0.10	35	40.757
85	10.83	+0.09	+0.31	+0.08	35	41.685
85	10.83	+0.10	+0.33	+0.10	20	50.740
86	10.11	−0.12	−0.07	−0.12	20	51.821
86	10.09	−0.11	−0.05	−0.14	20	52.794
86	10.11	−0.10	−0.07	−0.14	20	56.659
87	11.22	−0.09	+0.02	−0.12	20	52.811
88	10.79	+0.05	+0.27	−0.03	35	41.703
88	10.69	0.00	+0.21	+0.01	35	42.721
88	10.83	+0.02	+0.31	−0.01	35	43.818
88	10.82	0.00	+0.29	+0.02	35	44.666
88	10.82	+0.02	+0.32	−0.03	20	45.714
88	10.81	+0.02	+0.32	−0.03	20	46.742
88	10.78	+0.01	+0.23	+0.02	20	47.804
88	10.76	+0.03	+0.27	−0.04	20	49.736
88	10.75	+0.02	+0.28	0.00	20	50.752
88	10.74	+0.01	+0.32	−0.01	20	51.834
88	10.71	+0.04	+0.29	−0.01	20	52.834
88	10.72	+0.02	+0.30	−0.01	20	53.790
88	10.73	+0.02	+0.31	−0.01	20	54.586
88	10.71	+0.02	+0.31	−0.01	20	55.595
88	10.73	+0.02	+0.32	−0.01	20	56.679
89 + 90	10.84	−0.19	+0.05	−0.11	20	55.608
89 + 90	10.86	−0.19	+0.07	−0.09	20	56.689
92	9.71	+0.57	+0.53	+0.32	35	40.774
92	9.71	+0.58	+0.52	+0.32	35	44.685
92	9.71	+0.58	+0.54	+0.30	20	50.805
94	10.04	+0.74	+0.98	+0.83	35	40.827
94	10.07	+0.76	+1.00	+0.83	35	44.699
94	10.07	+0.78	+1.00	+0.86	20	50.817
98	10.59	+0.13	+0.13	+0.17	35	40.841
98	10.59	+0.11	+0.14	+0.14	35	44.713
98	10.56	+0.13	+0.15	+0.15	20	50.831
99	11.45	+0.26	+0.56	+0.20	20	52.848
99	11.45	+0.24	+0.56	+0.20	20	53.815
100	11.57	−0.01	+0.09	+0.08	20	53.827
100	11.56	−0.02	+0.08	+0.10	20	54.596
100	11.55	0.00	+0.10	+0.10	20	55.836
101	11.60	+0.06	+0.12	+0.04	20	53.840
101	11.61	+0.06	+0.13	+0.03	20	54.609
101	11.60	+0.06	+0.12	+0.04	20	55.847
103	9.91	−0.02	+0.10	0.00	35	40.857
103	9.90	−0.02	+0.10	0.00	35	44.731
103	9.89	−0.02	+0.09	0.00	20	50.773
104	11.27	+0.09	+0.16	+0.11	20	50.783
104	11.26	+0.09	+0.15	+0.11	20	53.854
104	11.26	+0.09	+0.16	+0.11	20	55.855

TABLE 4 (continued)

Star	*V*	*B–V*	*V–R*	*R–I*	D(″)	J. D. 2440500+
105	10.02	+0.20	+0.63	+0.64	20	54.633
105	10.02	+0.21	+0.61	+0.65	20	55.825
105	10.02	+0.22	+0.62	+0.63	20	56.746
107	11.18	−0.01	+0.06	−0.05	20	54.652
107	11.19	−0.02	+0.10	−0.03	20	55.637
110	10.41	+0.25	+0.32	+0.18	20	54.662
110	10.41	+0.25	+0.32	+0.18	20	55.653
110	10.41	+0.22	+0.32	+0.17	20	56.754
111	10.34	+0.12	+0.18	+0.13	35	41.726
111	10.33	+0.12	+0.17	+0.13	35	44.748
111	10.32	+0.12	+0.18	+0.13	20	51.845
112	11.16	−0.02	+0.07	−0.07	20	54.672
112	11.16	−0.02	+0.07	−0.08	20	55.660
112	11.17	−0.02	+0.08	−0.06	20	56.762
113	11.49	−0.12	+0.02	−0.07	20	54.680
113	11.45	−0.10	−0.01	−0.06	20	55.667
113	11.47	−0.09	0.00	−0.08	20	56.773
116	10.54	0.00	+0.16	0.00	20	47.834
116	10.54	0.00	+0.17	0.00	20	49.750
116	10.53	−0.01	+0.15	0.00	20	51.856
117	9.93	+1.05	+0.76	+0.52	35	41.742
117	9.91	+1.03	+0.74	+0.54	35	43.845
117	9.96	+1.03	+0.78	+0.53	35	44.763
118	9.88	+0.08	+0.13	+0.07	35	41.758
118	9.86	+0.08	+0.13	+0.07	35	42.808
118	9.91	+0.07	+0.15	+0.05	35	43.856
118	9.88	+0.06	+0.10	+0.09	35	44.804
119	10.81	+0.11	+0.20	+0.12	20	54.690
119	10.81	+0.11	+0.20	+0.12	20	55.674
120	10.88	+0.06	+0.12	+0.06	35	41.796
120	10.88	+0.03	+0.12	+0.08	35	42.792
120	10.91	+0.03	+0.14	+0.06	20	49.775
121	10.51	+0.10	+0.14	+0.06	35	41.811
121	10.51	+0.06	+0.14	+0.06	35	42.774
121	10.51	+0.08	+0.14	+0.06	20	49.790
123	10.67	+0.12	+0.45	+0.11	20	45.800
123	10.64	+0.11	+0.45	+0.11	20	46.841
123	10.64	+0.11	+0.45	+0.11	20	49.819
124	11.89	+0.10	+0.25	+0.14	20	54.703
124	11.84	+0.10	+0.23	+0.14	20	55.682
125	11.79	−0.04	+0.11	−0.05	20	54.713
125	11.77	−0.01	+0.11	−0.05	20	55.690
126	10.94	+0.16	+0.70	−0.06	20	45.819
126	10.94	+0.13	+0.70	−0.07	20	46.857
126	10.94	+0.15	+0.70	−0.06	20	49.835

TABLE 4 (continued)

Star	*V*	*B−V*	*V−R*	*R−I*	D(″)	J. D. 2440500+
127	11.16	−0.07	+0.17	−0.14	20	54.724
127	11.16	−0.06	+0.17	−0.13	20	55.700
127	11.17	−0.08	+0.17	−0.12	20	56.785
128	10.48	−0.07	+0.04	−0.06	20	54.734
128	10.47	−0.06	+0.02	−0.06	20	55.708
128	10.48	−0.06	+0.03	−0.06	20	56.793
129	11.32	0.00	+0.13	−0.07	20	54.755
129	11.32	+0.01	+0.09	−0.09	20	55.716
130	11.33	+0.18	+0.17	+0.11	20	54.765
130	11.33	+0.18	+0.17	+0.11	20	55.723
130	11.37	+0.15	+0.20	+0.11	20	56.802
131	10.20	+0.37	+0.40	+0.30	20	54.773
131	10.22	+0.37	+0.40	+0.30	20	55.730
131	10.22	+0.37	+0.40	+0.30	20	56.810
136	9.15	+0.16	+0.31	+0.22	20	54.782
136	9.15	+0.16	+0.32	+0.20	20	55.737
136	9.15	+0.18	+0.32	+0.21	20	56.817
144	11.11	−0.12	+0.14	0.00	20	54.789
144	11.11	−0.12	+0.14	0.00	20	55.753
148	11.94	+0.26	+0.51	+0.22	20	54.801
148	11.94	+0.26	+0.50	+0.22	20	56.834
149	12.28	−0.06	+0.20	−0.18	20	54.811
149	12.28	−0.06	+0.20	−0.18	20	55.773
149	12.24	−0.02	+0.19	−0.17	20	56.842
150	9.93	+0.94	+0.72	+0.43	35	41.848
150	9.94	+0.90	+0.73	+0.43	35	42.850
150	9.94	+0.97	+0.72	+0.43	20	47.847
151	10.74	+0.33	+0.33	+0.33	20	54.819
151	10.74	+0.36	+0.33	+0.33	20	55.783
152	11.19	+0.05	+0.16	+0.05	20	54.827
152	11.20	+0.05	+0.16	+0.05	20	55.792
153	10.34	+0.23	+0.29	+0.22	35	41.859
153	10.32	+0.26	+0.29	+0.21	35	42.863
153	10.33	+0.25	+0.27	+0.21	35	44.820
153	10.33	+0.25	+0.28	+0.20	20	49.849
154	11.98	+0.12	+0.18	+0.09	20	54.836
154	12.01	+0.07	+0.19	+0.08	20	55.803
154	12.01	+0.10	+0.18	+0.07	20	56.851
155	11.61	−0.08	+0.07	−0.11	20	54.847
155	11.61	−0.06	+0.07	−0.09	20	55.814
156	11.63	−0.07	+0.25	+0.31	35	42.684
156	11.63	−0.06	+0.30	+0.31	35	43.707

TABLE 4 (continued)

Star	*V*	*B–V*	*V–R*	*R–I*	D(″)	J. D. 2440500+
156	11.77	+0.05	+0.06	+0.01	20	45.728
156	11.79	+0.07	+0.06	−0.01	20	46.709
157	10.84	+0.26	+0.42	+0.53	35	42.702
157	10.84	+0.26	+0.47	+0.55	35	43.723
157	11.10	+0.23	+0.41	+0.65	20	45.746
157	11.12	+0.23	+0.45	+0.63	20	47.733
158	10.01	+0.16	+0.49	+0.52	35	42.744
158	10.05	+0.16	+0.53	+0.53	35	44.649
158	10.24	+0.27	+0.56	+0.65	20	45.783
158	10.26	+0.27	+0.58	+0.65	20	50.846

III. Two Color Diagrams

The analysis of the *BVRI*-photometry contained in Tables 3 and 4 could include various comparisons of the several color indices. We have shown (Mendoza 1967*a*, 1969 *a*) that *V—R versus B—V* is a very useful two color diagram. Thus, in Figure 7 we have plotted *V—R versus B—V* for

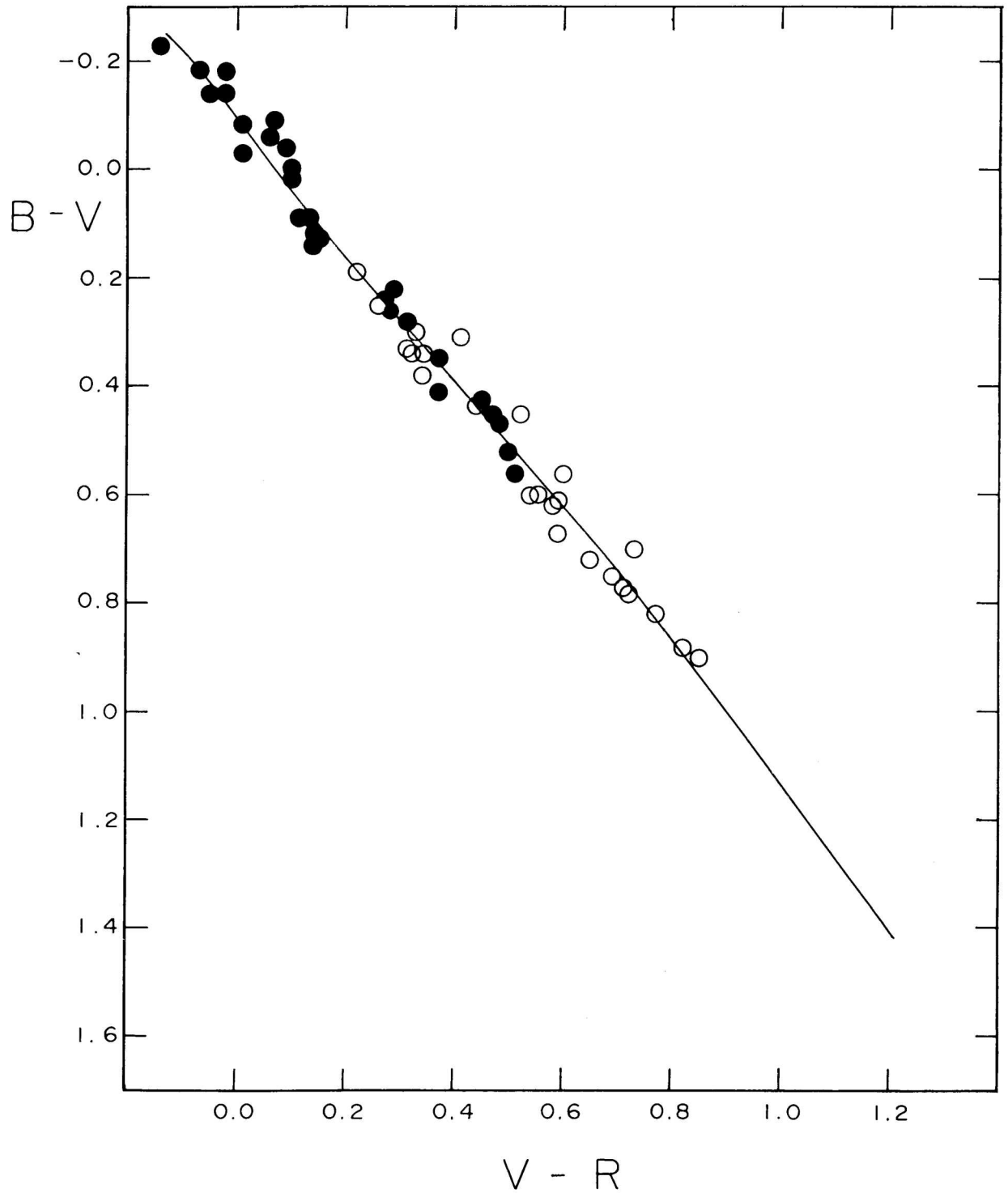

Fig. 7.—*The* (V—R, B—V) *diagram for galactic supergiants. (B0—A5). The open circles represent stars of the double cluster h and χ Persei; and the filled circles, other supergiant stars which are listed in the Bright Star Catalogue. The slanting line is a "visual" mean line which represents the standard* (V—R, B—V) *relation for galactic supergiant stars (B0—A5).*

the galactic supergiants. The photometry has been taken from Mendoza (1967*c*) for the supergiants of the double cluster, h and χ Persei, and from Johnson, Mitchell, Iriarte, and Wisniewski (1966) for other supergiant stars, listed in the Bright Star Catalogue (Hoffleit 1964). All the galactic supergiant stars plotted in Figure 7 define a smooth curve represented by a slanting line, which we may assume is the *(V—R, B—V)* standard relation for galactic supergiant stars of spectral type from B0 to A5. The *(V—R, B—V)* diagram for the Small Magellanic Cloud is shown in Figure 8. It is remarkable how all the SMC objects (except the two Harvard variables) lie well above the line defined by galactic supergiants. The mean distance from the line is around 0.15 mag. It is interesting to

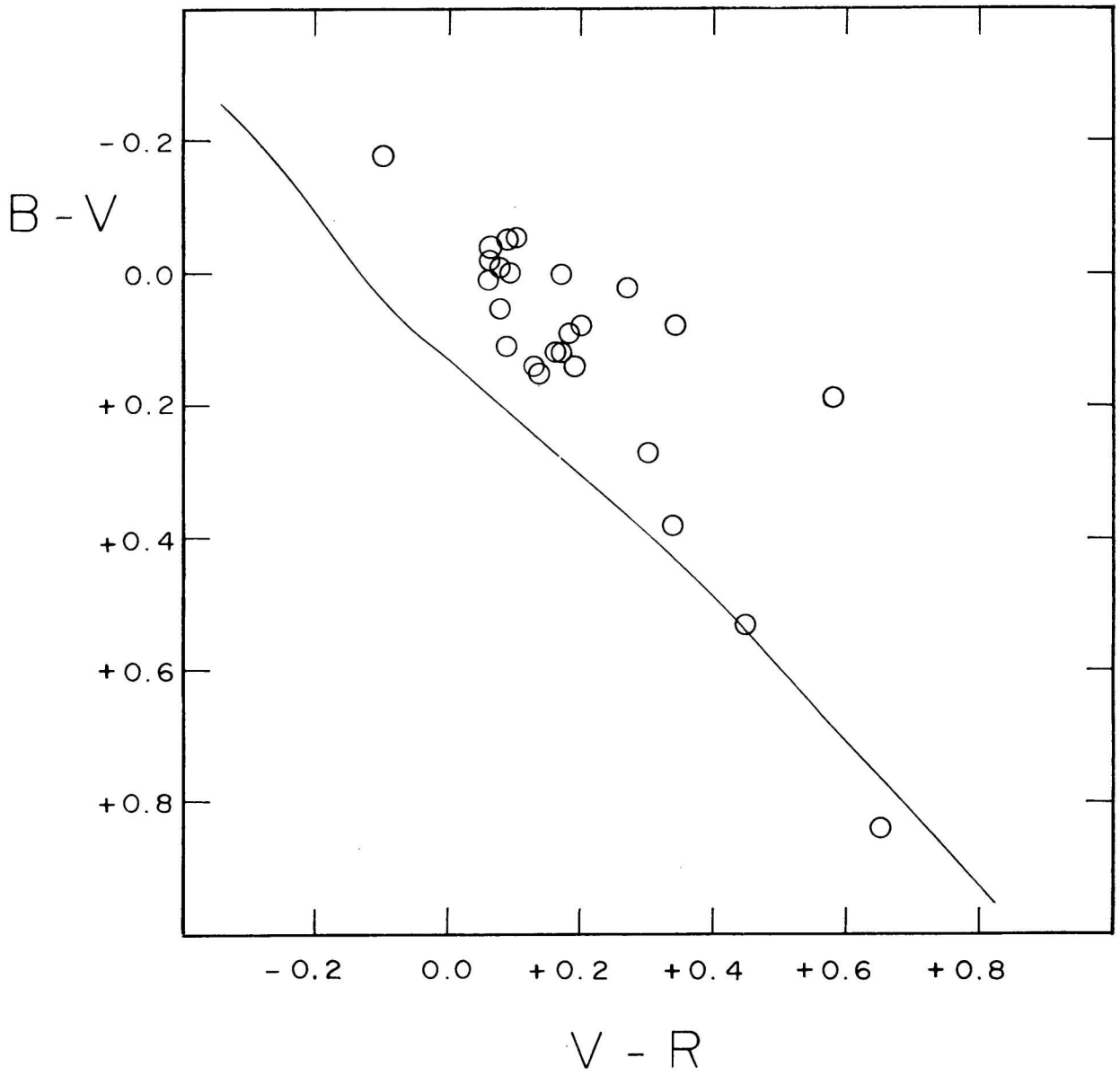

Fig. 8.—*The* (V—R, B—V) *diagram of stars that belong to the Small Magellanic Cloud. The slanting line represents the* (V—R, B—V) *"standard" relation of galactic supergiant stars (B0—A5).*

point out that in a *(V—R, B—V)* color diagram the 0f and B_e (shell) stars and T Tauri-like objects lie above the line defined by the main sequence of unreddened galactic clusters (Mendoza 1969*a*). It has been shown (Mendoza 1966, 1968) that these objects have infrared excesses. Now, the B0-A5 galactic supergiant stars studied (Mendoza 1969*a*) neither do lie above the Hyades main sequence nor have infrared excesses, other than that by interstellar extinction. Figure 9 is the *(V—R, B—V)* diagram for the Large Magellanic Cloud. The LMC objects have the same characteristic shown by the SMC stars, namely, most stars lie well above the *(V—R, B—V)* standard line defined by the galactic supergiants. Again, the F8-G5 objects are located below the line.

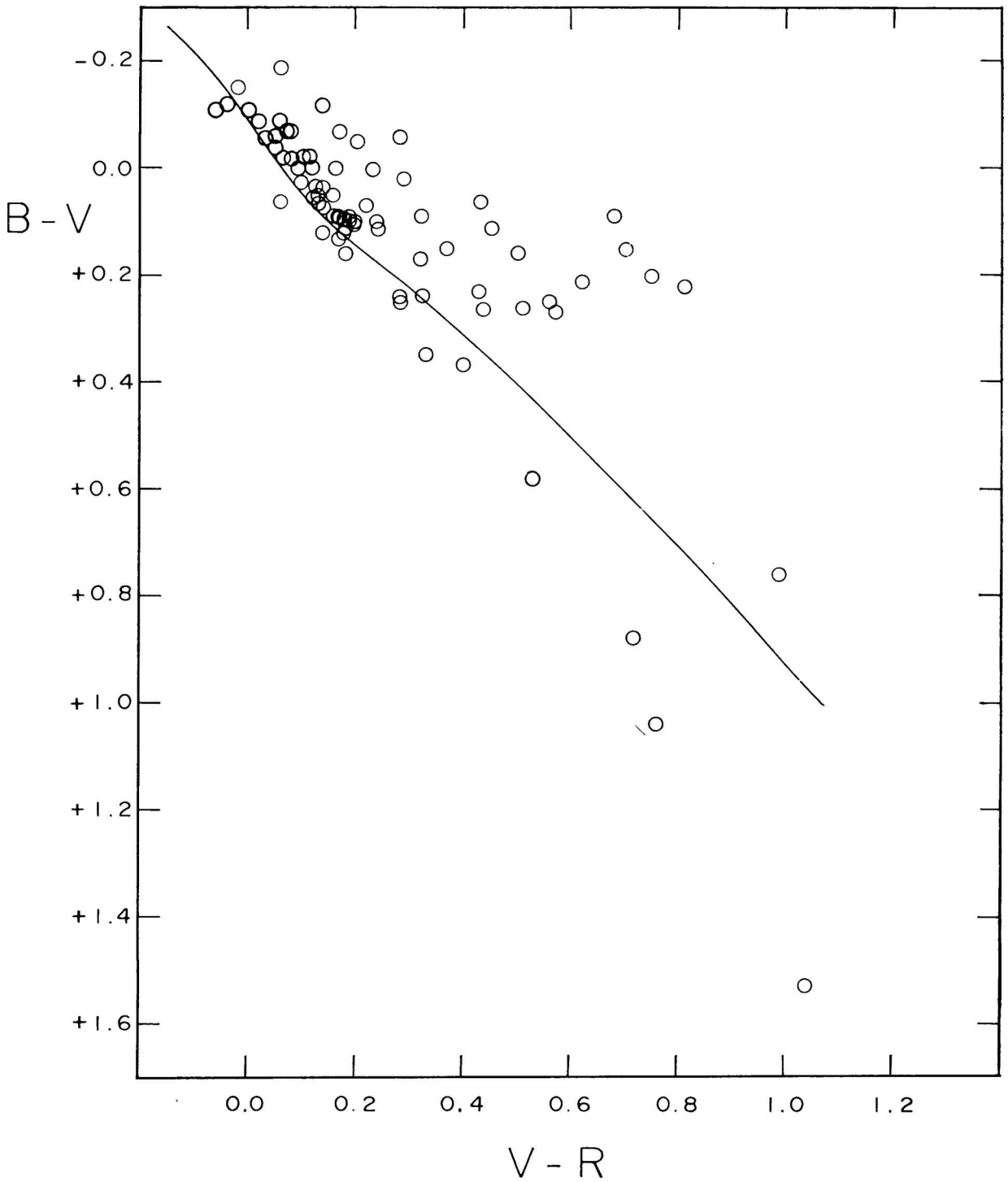

Fig. 9.—*The* (V—R, B—V) *diagram of stars that belong to the Small Magellanic Cloud. The slanting line represents the* (V—R, B—V) *"standard" relation of galactic supergiant stars.*

Another two color diagram, that of *V—R versus R—I* is shown in Figures 10-12. Figure 10 is for the same galactic supergiant stars given in Figure 7. Again, we may assume that the slanting line drawn in Figure 10 represents the *(V—R, R—I)* standard relation for galactic supergiant stars. Next, we construct the same type of diagram for the SMC (Fig. 11). In Figure 11 the scatter is larger than in Figure 10; the circle that lies furthest from the line represents a peculiar object. The objects below the line are B6-A3 stars. Figure 12 shows the *(V—R, R—I)* diagram of objects

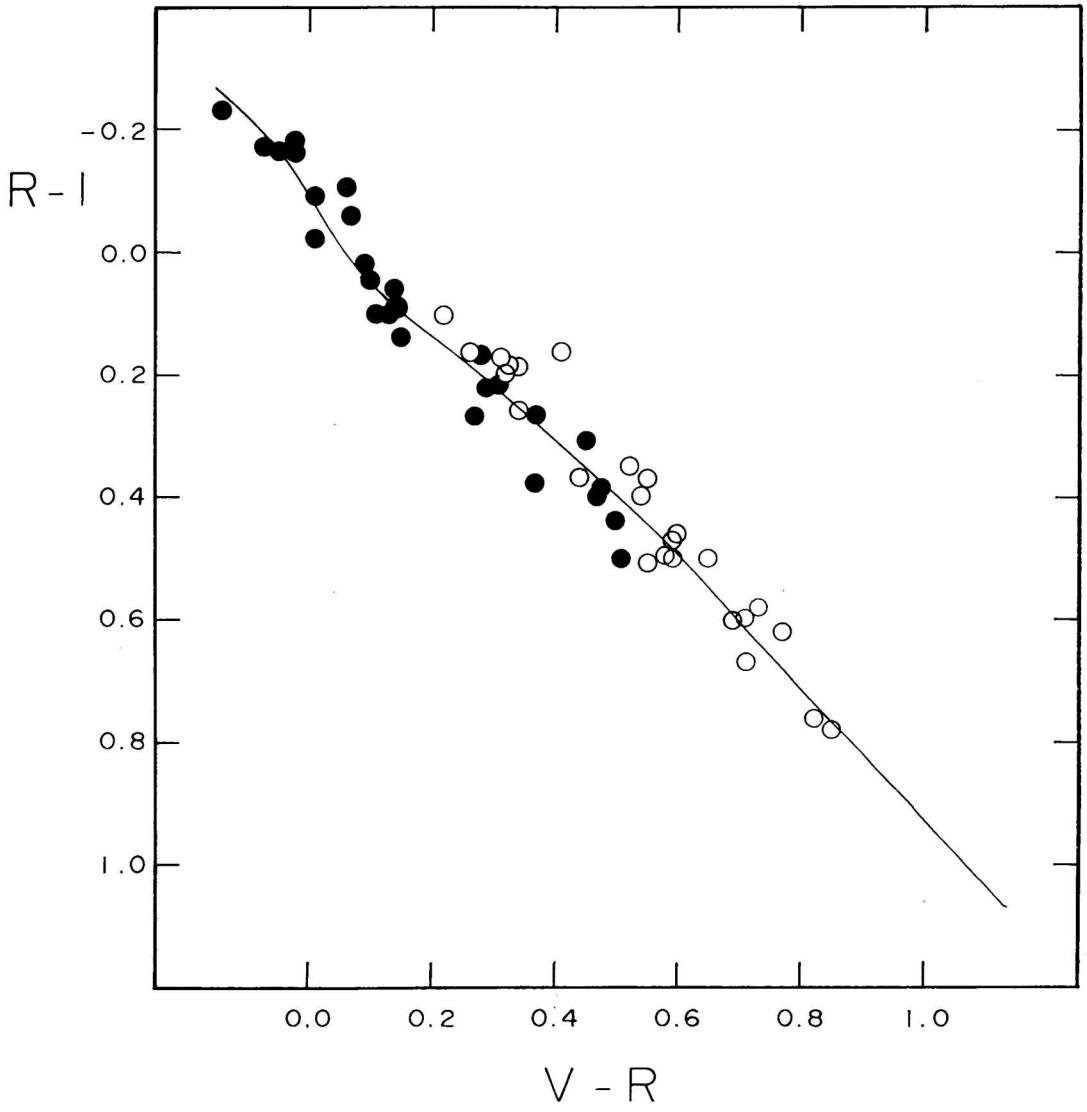

Fig. 10.—*The* (V—R, R—I) *diagram for galactic supergiant stars (B0—A5). The symbols represent the same objects as in Fig. 7.*

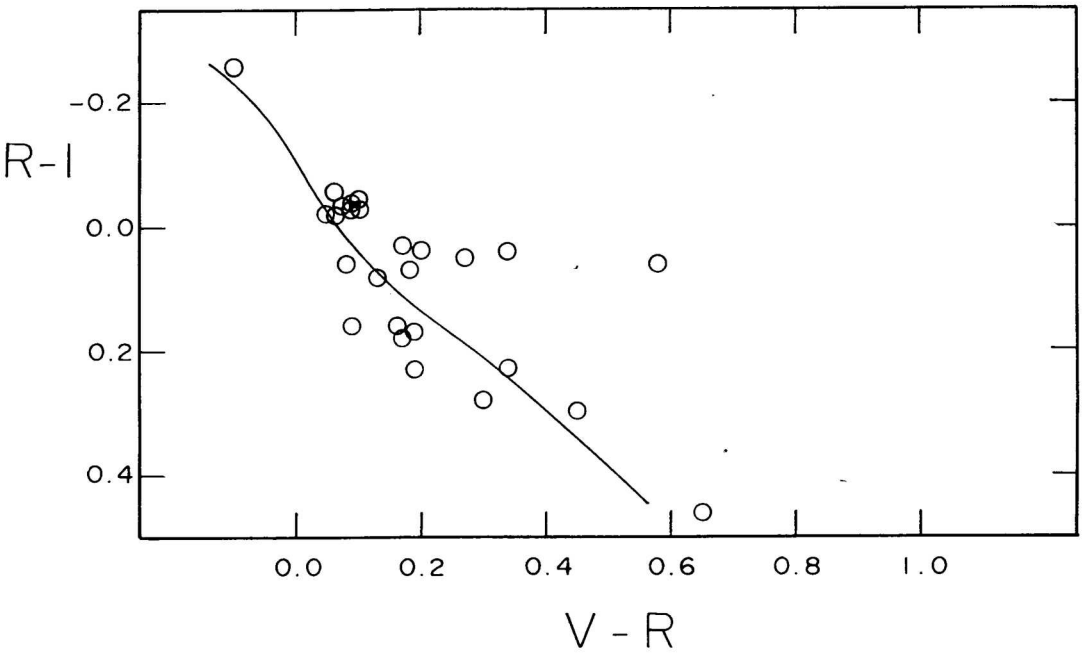

Fig. 11.—*The* (V—R, R—I) *diagram of stars that belong to the Small Magellanic Cloud. The slanting line represents the* (V—R, R—I) *"standard" relation of galactic supergiant stars (B0—A5).*

that belong to the Large Magellanic Cloud. Again peculiar and nebular objects lie above the *(V—R, R—I)* standard relation line, valid for galactic supergiant stars.

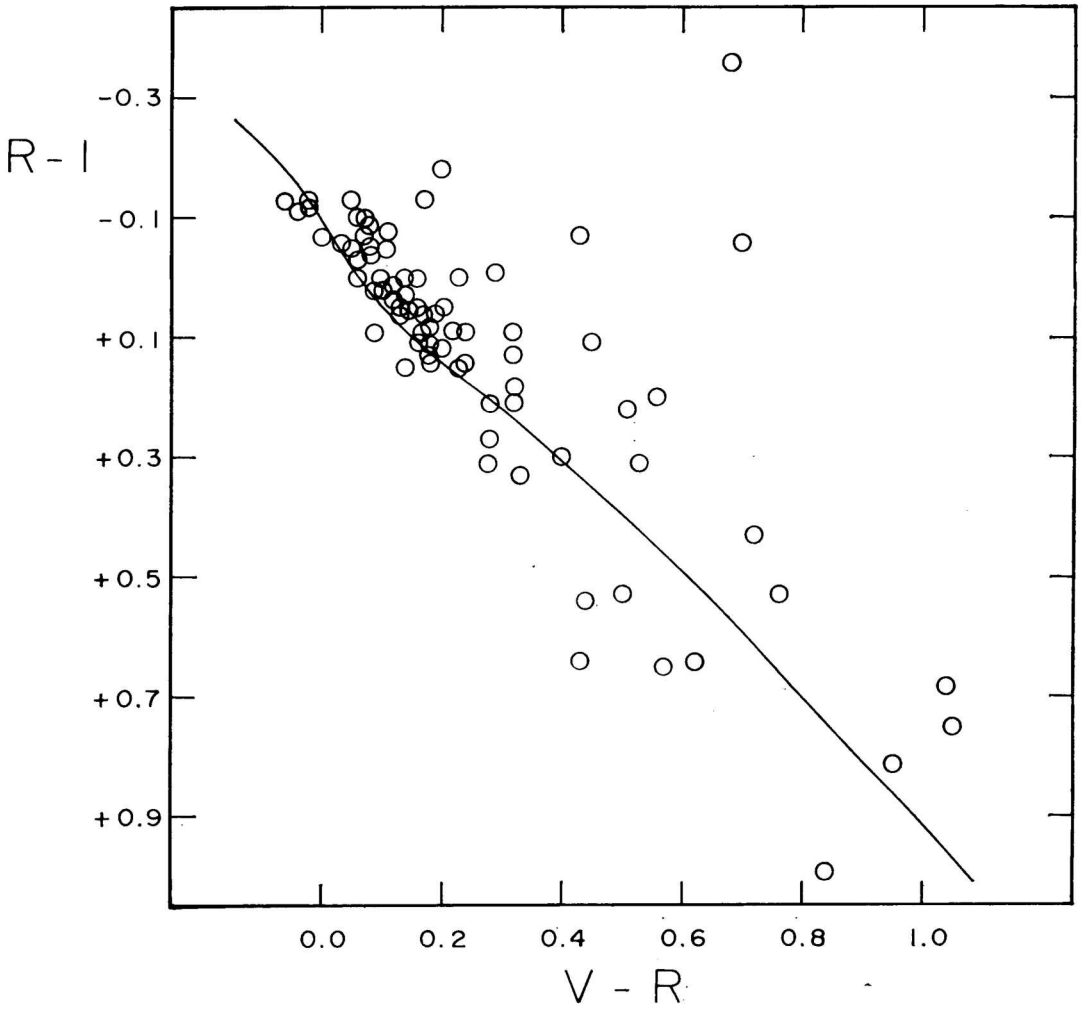

Fig. 12.—*The* (V—R, R—I) *diagram of stars that belong to the Large Magellanic Cloud. The slanting line represents the* (V—R, R—I) *"standard" relation of galactic supergiant stars.*

IV. Interstellar Extinction

A combination of the photometry and spectral types given in Table 3 can give the color excesses of objects from the Magellanic Clouds. Using only those stars that do not show spectral peculiarities, emission lines or nebulosity, we find that the color excesses are smaller than those found in most galactic supergiants. Figure 13 shows the relation between spectral type (B0-A5) and the *V—R* color excess normalized to the *B—V* color excess (E_{V-R}/E_{B-V}) for galactic supergiant stars. In this Figure we notice that supergiants of the double cluster, h and χ Persei, show smaller scatter than BS-supergiants because the former are more reddened than the latter and the ratio E_{V-R}/E_{B-V} has a small dispersion when E_{B-V} is large. Figure 13 also shows that stars earlier than B6 lie above the theoretical value of van de Hulst (1949) and those later than B6 lie below this value. However, the average color excess ratio from B0 to A5 does not differ appreciable from $E_{V-R}/E_{B-V} = 0.80$, van de Hulst's value. Figure 14 shows the (Sp, E_{V-R}/E_{B-V}) relation for Magellanic Cloud objects. It should be pointed out that these stars have smaller reddening than most of the supergiants of h and χ Persei, thus we should expect a scatter similar to that of BS-supergiants; many Magellanic Cloud objects do show it. However, the stars around A0 type lie systematically below the van de Hulst's value by such a large amount that it cannot be explained by a poor determination of the E_{V-R}/E_{B-V} ratio.

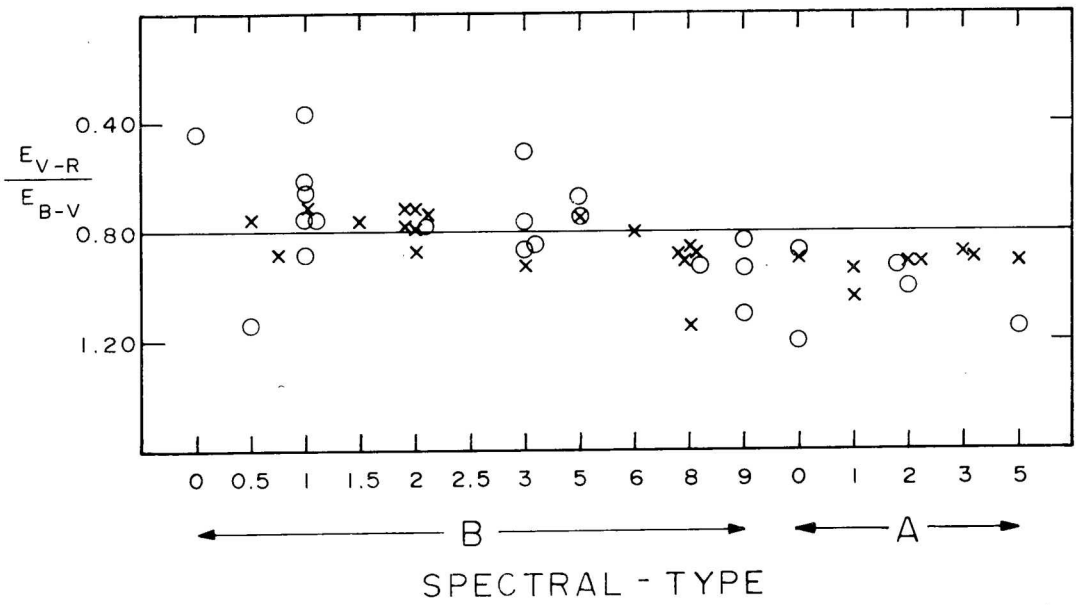

Fig. 13.—*The spectral type-color excess relation for galactic supergiant stars (B0—A5). Crosses represent supergiant stars that belong to h and χ Persei; open circles, BS-supergiants. The ordinates give the color excess in* V—R *normalized to the color excess* B—V. *The solid line represents the value given by van de Hulst (1949).*

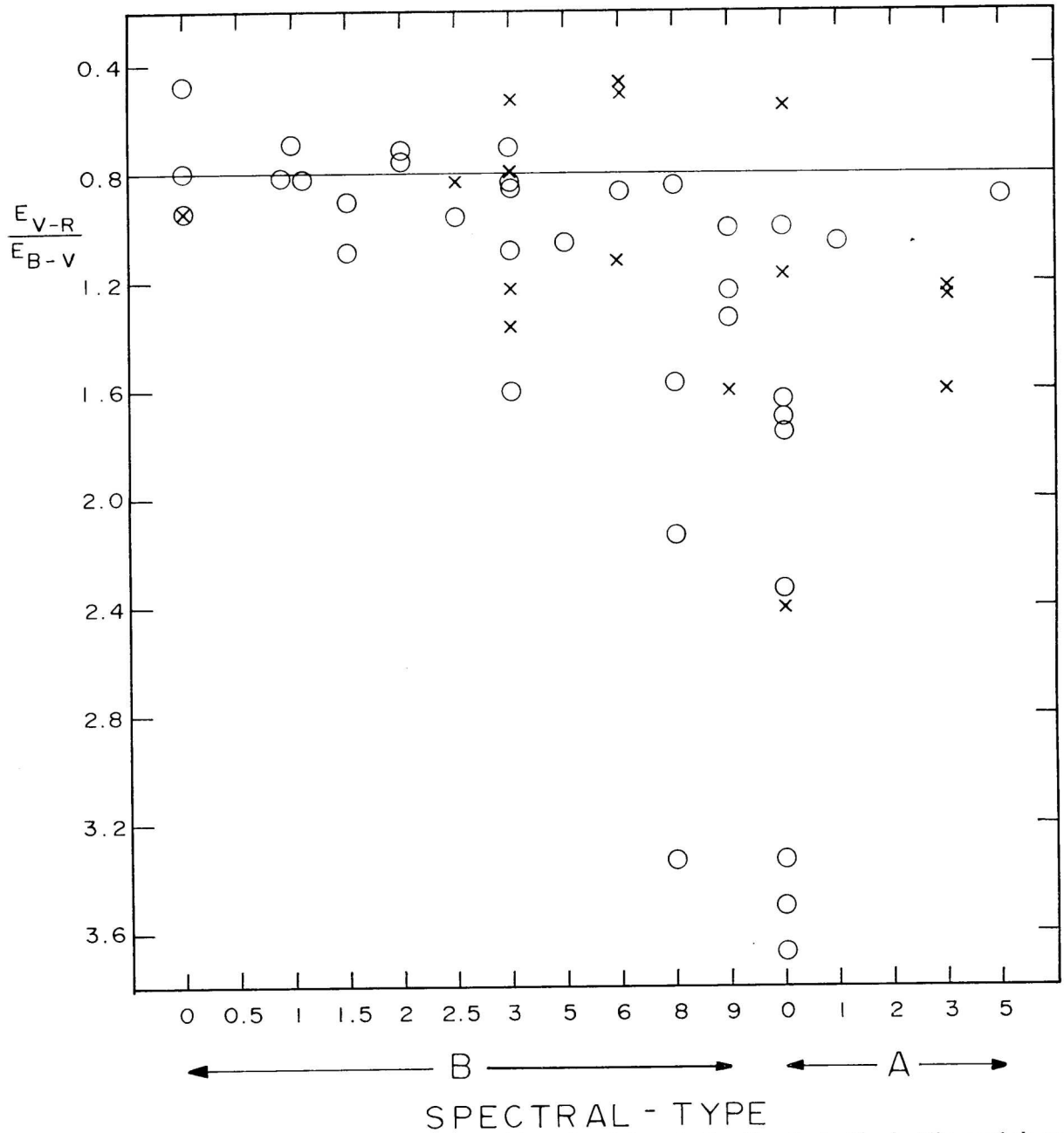

Fig. 14.—*The spectral type-color excess relation for objects that belong to the Magellanic Clouds. The symbols represent: crosses, SMC stars; open circles, LMC stars; the solid line, the value given by van de Hulst. The ordinates are the same as in Fig. 13.*

Figure 15 shows the (Sp, E_{R-I}/E_{B-V}) relation for galactic supergiant stars. In this figure the slope indicated by the observations is nearly zero and on the average the stars lie about 0.05 units above the theoretical value of van de Hulst (1949). Figure 16 shows the (Sp, E_{R-I}/E_{B-V}) relation for

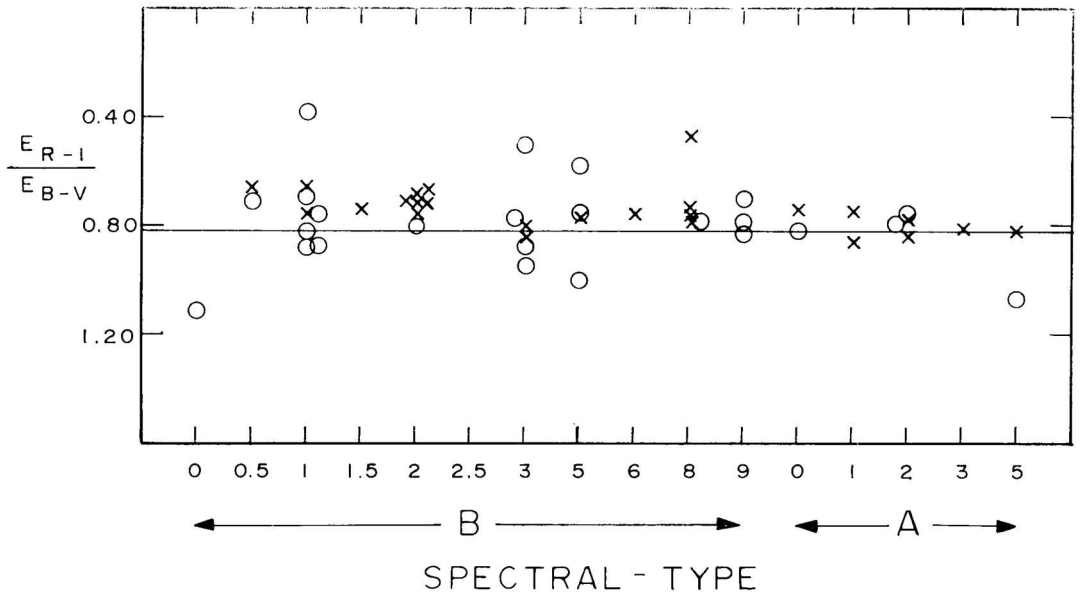

Fig. 15.—*The spectral type-color excess relation for galactic supergiant stars (B0—A5). The symbols are those of Fig. 13. The ordinates give the color excess in* R—I *normalized to* E_{B-V}.

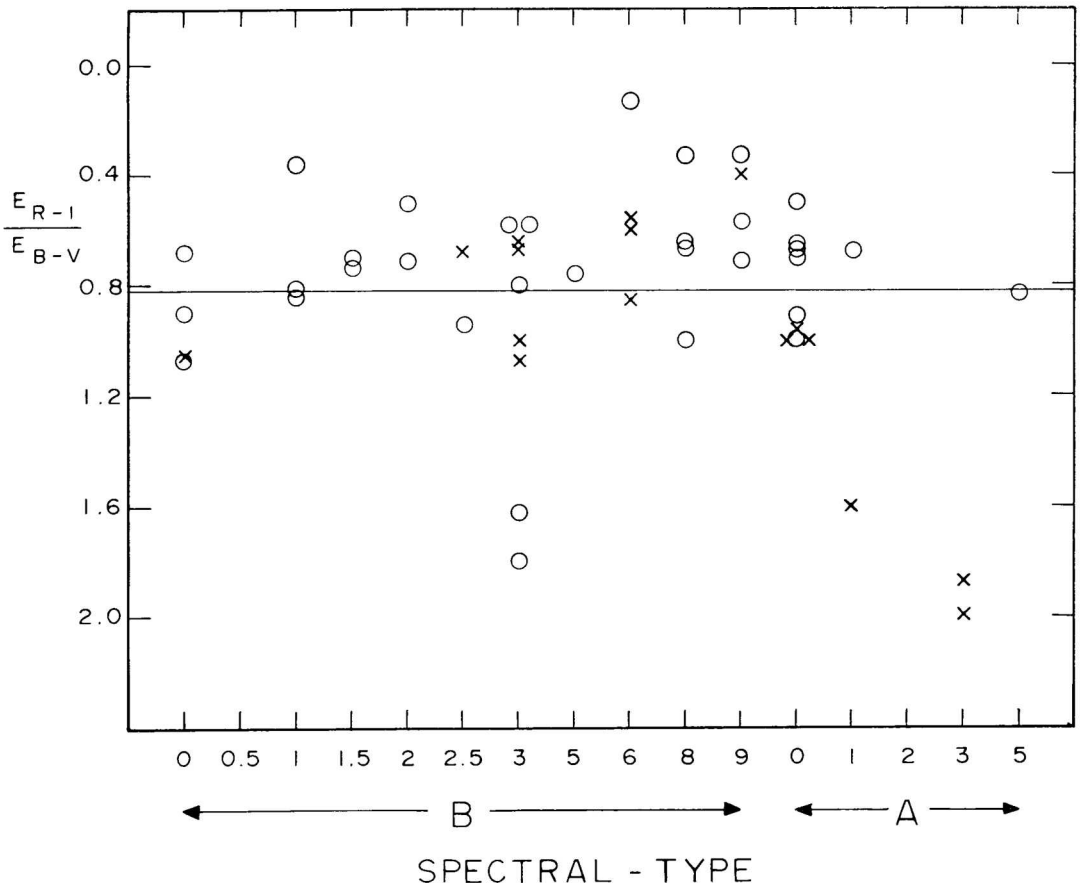

Fig. 16.—*The spectral type-color excess relation for objects that belong to the Magellanic Clouds. The symbols are those of Fig. 14. The ordinates are the same as in Fig. 15.*

Magellanic Cloud objects. The scatter shown in this diagram is large. However, it is approximately four times larger above the line defined by the galactic supergiants (see Fig. 15) than below it, except for the B3 and A3 stars which mostly are located underneath. Of the B6-A0 objects, 70% lie above the theoretical line.

The color excesses can be used to compute the total absorption. Let us assume that the ratio of total to selective extinction is $\frac{A_V}{E_{B-V}} = 3.3$, $\frac{A_V}{E_{V-R}} = 3.6$ and $\frac{A_V}{E_{R-I}} = 4.4$ (Mendoza 1968). For the time being, let us also assume that $V_o = V - A_v$ where A_v is the mean value obtained from the above three A_v's. The results are shown in Figures 17 and 18; they represent the Hertzsprung-Russell diagram for the B0-A5 stars of the Magellanic Clouds. A comparison of Figures 17 and 18 indicates a difference in the distance moduli of the clouds of approximately 0.25 mag. in excellent agreement with other determinations (Bok 1966). This difference implies that the Large Cloud is closer to us than the Small Cloud by this amount.

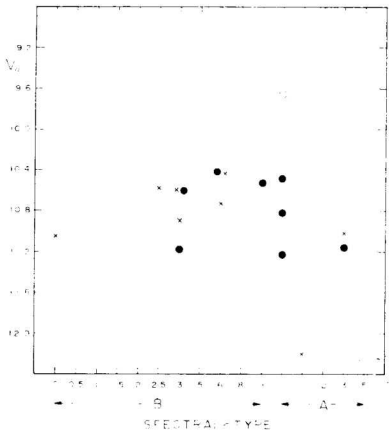

Fig. 17.—*The Hertzprung-Russel diagram for the Small Magellanic Cloud. The ordinates give the V_o's "corrected" for interstellar extinction. The symbols represent: open circles, luminosity Ia-0; filled circles, luminosity Ia; and crosses, luminosity I.*

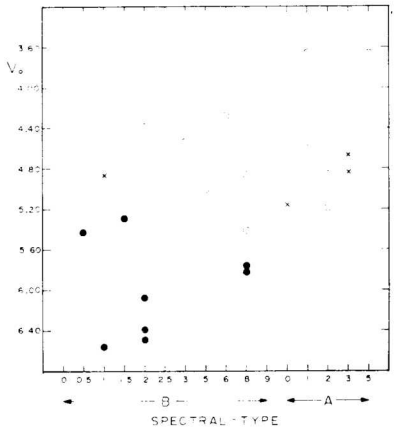

Fig. 18.—*The Hertzprung-Russell diagram for the Large Magellanic Cloud. The ordinates give the V_o's "corrected" for interstellar extinction. The symbols represent: open circles, luminosity Ia-0; filled circles, luminosity Ia; and crosses, luminosity I.*

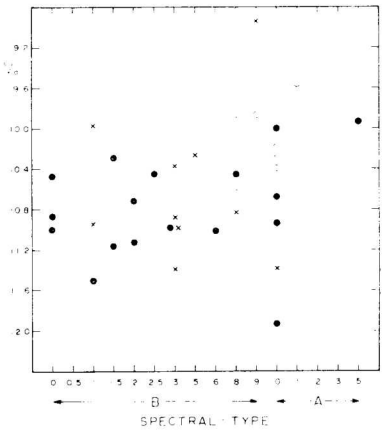

Fig. 19.—*The Hertzprung-Russell diagram for the h and χ Persei. The symbols represent: open circles, luminosity Ia; the largest open circle, two stars; filled circles, luminosity Ib; crosses, luminosity Iab.*

V. Conclusions

A comparison of the Hyades main sequence (Mendoza 1967*c*), the galactic supergiant stars (Fig. 10) and the Magellanic Cloud objects (Figs. 11 and 12) indicates that the *(V—R, R—I)* diagram is sensitive to the luminosity. The galactic supergiants lie below the Hyades main sequence and many Magellanic Cloud objects lie below the galactic supergiant sequence. Thus, we may state that the photometry presented in Tables 3 and 4 indicates the existence of "super-supergiant" objects in the Clouds, this is to say, they are more luminous than the most luminous observed galactic stars. Because of the large range in luminosities among some galactic supergiants and some Magellanic Cloud objects, perhaps of five magnitudes or even more, it is difficult to apply the photometric method (Mendoza 1967*c*) to derive the distance to the Clouds. A comparison of the Hertzprung-Russell diagram for the Large Magellanic Cloud and the double cluster, h and χ Persei, indicates that the distance modulus of LMC should be larger than 18.0 mag. Figure 19 shows the Hertzprung-Russell diagram of the B0-A5 supergiants in h and χ Persei, computed under the same assumptions as those of the clouds.

The *(V—R, B—V)*, (Sp, E_{V-R}/E_{B-V}) and (Sp, E_{R-I}/E_{B-V}) diagrams (Figs. 8, 9, 14 and 16) can be interpreted as evidence of color excesses in *V—R* for many Magellanic Cloud objects unexplained by interstellar extinction alone. Most of the stars of spectral type around A0 fall in this group. There are many possible explanations for the additional flux in the red wavelength: *a)* emission line radiation in the object's neighborhood; *b)* free-free radiation in the stellar vicinity; *c)* a peculiar extinction law. These three causes may be ruled out because it seems that the anomalous *V—R* color excess is more sensitive to .spectral type rather than to sky position. *d)* Incorrect intrinsic colors. Since the intrinsic colors used here for the supergiants in the Galaxy are reasonably accurate for the spectral range B0-A5 as well as for a number of Magellanic objects of different spectral types

thus it is difficult to expect them to be wrong by the large factor needed in some instances to remove the discrepancies. *e)* Anomalous stellar emission. This perhaps would explain those objects with emission lines, but hardly those shown in Figure 14. *f)* Late type companions. The great majority of the stars with anomalous red excesses does not show the $R-I$ excess which should be present if a red companion exists, thus we also can eliminate this possibility as the main cause of the $V-R$ color excesses. *g)* Circumstellar dust clouds; and *h)* different atmospheric chemical composition between stars in the Clouds and in the Galaxy. At present we do not have means to dispose of these last two possibilities, therefore one or the other, or both could be responsible for the additional red radiation.

It is known that the H/H_e ratio is approximately the same in the Galaxy and the Magellanic Clouds (cf. Peimbert and Spinrad 1970). Therefore, if there is a difference in the chemical composition of the atmospheres of Magellanic Cloud objects and galactic supergiant stars then it would be in the metal content; probably being lower in the Clouds than in the Galaxy. We know that dust re-radiation is present in a number of stars in the Galaxy; thus, this could be the most likely explanation for the excess radiation in R. This can be confirmed by the infrared photometry of these objects. However, it should be pointed out again that galactic stars classified as Ia, Iab and Ib (types B0-A5) show color excesses in $V-R$ which are explained by interstellar extinction alone (Mendoza 1969*a*).

Hence we conclude that some Magellanic Cloud objects differ, at least in two aspects, from galactic supergiant stars. They are more luminous than the most luminous galactic supergiants and they have an additional radiation in the red region; the latter is probably caused either by a dust circumstellar envelope or by a different atmospheric chemical composition, or by both.

We are indebted to Dr. V. M. Blanco for making available the facilities at Cerro Tololo Inter-American Observatory, to Dr. H. L. Johnson for the use of the red photometer, to Dr. S. Torres-Peimbert for reading the manuscript and to Miss. T. Gómez for inking the figures and typing the manuscript.

REFERENCES

Arp, H. C. 1958, *A. J.* **63,** 118.
Bok, B. J. 1966, *Ann. Rev. Astr. and Ap.*, **4,** ed. L. Goldberg (Palo Alto, Calif.: Annual Reviews) p. 95.
Feast, M. W., Thackeray, A. D., and Wesselink, A. J. 1960, *M. N. R. A. S.*, **121,** 337.
Henize, K. G. 1956, *Ap. J. Suppl.* **2,** 315.
Hoffleit, D. 1964, *Catalogue of Bright Stars* (New Haven, Conn.: Yale University Observatory).
Hulst, H. C. van de 1949, *Rech. Astron. Obs. Utrecht,* **11,** (Part 1).
Johnson, H. L. 1964, *Bol. Obs. Tonantzintla y Tacubaya,* **3,** 305.
Johnson, H. L., Mitchell, R. I., Iriarte, B., and Wisniewski, W. Z. 1966, *Comm. Lunar and Planetary Lab.*, **4,** 99.
Mendoza, E. E. 1963, *Bol. Obs. Tonantzintla y Tacubaya,* **3,** 137.
———. 1966, *Ap. J.*, **143,** 1010.
———. 1967*a*, *Bol. Obs. Tonantzintla y Tacubaya,* **4,** 106.
———. 1967*b*, *Bol. Obs. Tonantzintla y Tacubaya,* **4,** 114.
———. 1967*c*, *Bol. Obs. Tonantzintla y Tacubaya,* **4,** 149.
———. 1968, *Ap. J.*, **151,** 977.
———. 1969*a*, *P. D. A.* (Univ. Chile), **1,** 106.
———. 1969*b*, *Bol. Obs. Tonantzintla y Tacubaya,* **5,** 104.
———. 1970, *Bol. Obs. Tonantzintla y Tacubaya,* **5,** 209.
Peimbert, M., and Spinrad, H. 1970, *Astron. and Astrophys.* **7,** 311.
Westerlund, B. E., Danziger, J., and Graham, J. 1963, *Observatory,* **83,** 74.